IEEE Access
Multidisciplinary | Rapid Review | Open Access Journal

Received July 17, 2019, accepted August 8, 2019, date of publication August 13, 2019, date of current version August 30, 2019.

Digital Object Identifier 10.1109/ACCESS.2019.2935015

H-Infinity Control for T-S Aero-Engine Wireless Networked System With Scheduling

BIN ZHOU[1], SHOUSHENG XIE[1], AND JUNHUA HUI[2]
[1]Aeronautics and Astronautics Engineering College, Air Force Engineering University, Xi'an 710038, China
[2]College of Information and Communication, National University of Defense Technology, Changsha 410073, China

Corresponding author: Bin Zhou (icy_sky@foxmail.com)

This work was supported by the National Natural Science Foundation of China under Grant 51606219 and Grant 51476187.

ABSTRACT Nonlinear control and signal scheduling are the two difficulties for wireless networked control application in aero-engine. For aero-engine nonlinear complex flight conditions, the co-design of dynamic scheduling and robust H-infinity control method analysis was conducted by employing a class of aero-engine T-S (Takagi-Sugeno) fuzzy model based on flight envelop division. For each state space model of the fuzzy rules, the sufficient condition for the asymptotically stability of robust H-infinity controller design under MEF-TOD (Maximum Error First-Try Once Discard) scheduling strategy based on the Lyapunov function and switched system theory is deduced. Then the global fuzzy controller strategy was identified based on the parallel distributed compensation technology, which shares the same fuzzy rules with the T-S model. Finally, a TrueTime simulation example demonstrates the efficiency of the proposed method.

INDEX TERMS Aero-engine, H-infinity control, networked control, scheduling.

I. INTRODUCTION

As the approach of 5G era, wireless communication technology has received further sustainable development. In order to reduce the weight of aircrafts and avoid the unreliability of electric transmission media, the application of wireless control on aircrafts is the inevitable development trend. Once wireless communication is used, anti-interference capability and low bandwidth coping ability will become the first problem to be resolved as fast as possible. If network cannot run smoothly, signal scheduling must be active to ensure the control performance, thus, it is of great significance for the embedded design of scheduling strategy to nonlinear control.

At the present time, the adopted aero-engine controllers are still in the process of linear control and centralized control, which change the parameters for different flight conditions. Huge strides over the past decades in aerothermodynamics and material have improved engine performance and efficiency to an unprecedented degree, which on the other hand challenges the capability of control systems. Because of the complicated flight condition in the large flight envelop, complex wireless network constraints, disturbance, control system uncertainties always become more severe.

The associate editor coordinating the review of this article and approving it for publication was Ivan Wang-Hei Ho.

For aero-engine controller design, flight envelop division is a common method to obtain multiple regions on the condition that certain performance indicators can be satisfied. Representative nominal working point from every region is chosen to build every small deviation state space model and design the corresponding controller. However, when the chosen working point is far away from the designed point, larger deviation will occur in the actual aero-engine working performance. Additionally, the aero-engine working condition will change complexly, inevitably arising system uncertainties such as parameter perturbations and outer disturbance, which has strong nonlinear characteristic and great influence on the adaptive capacity of controller to flight envelop regions. Furthermore, for aero-engine networked control system, problems of scheduling strategy and packet dropout, etc. cannot be ignored, so the controller design for nonlinear uncertain network-constrained system has become research hotspot in this field.

Currently in NCS (Networked Control System) research, reference [1] investigated the filtering problem for nonlinear NCS with time-varying delays. Reference [2] designed the H-infinity controller of NCS under denial-of-service jamming attacks. Reference [3] considered periodic event-triggered control for NCS with packet dropout and time delay. Reference [4] addressed H-infinity observer-based sliding mode control for linear NCS with event-triggered scheduling.

Reference [5] proposed a predictive control method for flight NCS with packet dropout and uncertainties. Reference [6] considered with an improved event-triggered control for with resource constraints. Reference [7] proposed a hybrid scheduling method for NCS with packet dropout. Thus, nonlinear NCS together with active scheduling will be research hotspot in the NCS application area, especially in WNCS (Wireless Networked Control System) area.

As an essential nonlinear modeling method, T-S fuzzy model can approach nonlinear function at any precision on in the real space [8]. Subsequent structure of the model is local linear system, which is convenient for stability analysis using linear methods, so T-S receives attention in nonlinear modeling. Although dynamic process can be reproduced accurately by only using T-S model in aero-engine controller design, model error caused by some network uncertainties cannot be eliminated completely. Therefore, it can be more pragmatic and robust for the embedded design of real time scheduling strategy to H-infinity control in the nonlinear T-S aero-engine networked system.

Recently, reference [9] adopted nonlinear H-infinity control theory to design the optimal controller for active magnetic bearing systems. Reference [10] proposed a power modulation controller based on the H-infinity design methodology. Reference [11] put forward an H-infinity active vibration control technique for a piezoelectric actuator. However, few researches can be found analyses both nonlinearity and signal scheduling in H-infinity controlling. Reference [12] analyzed dissipative-based fuzzy integral sliding mode control of continuous-time T-S fuzzy systems. Reference [13] focused on the observer-based output feedback control of T-S fuzzy systems. Reference [14] designed the event-triggered dynamic output feedback controller for T-S fuzzy systems under asynchronous network communications. However, few researches can be found considers with signal scheduling for the T-S fuzzy systems, especially in aero-engine networked system. Reference [15] investigated the optimal attack schedule in the wireless networked control system with multiple subsystems. Reference [16] presented a dynamic reconfiguration technique for the real-time scheduling. Reference [17] maximized the overall system performance based on the optimized periods and deadlines. However, the embedded of scheduling strategy into nonlinear control algorithms needs further investigation. In summary, it is necessary to design nonlinear controllers with network parameters for the future aero-engine ZigBee wireless NCS application considering with: 1) nonlinear system; 2) combined scheduling of input and output signals; 3)disturbing contained; 4) simulation switching technique of single-channel and multi-channel; and 5) aero-engine control application within the full flight envelop.

Considering the future trend of wireless communication and nonlinear control in the field of aviation and aerospace, this paper proposes a nonlinear T-S H-infinity control method embedded with TOD scheduling strategy based on the flight envelop division. Firstly, on each flight envelop point, the employed aero-engine T-S fuzzy model with the co-design of nonlinear state space equation and TOD scheduling algorithm is constructed. Then, the robust H-infinity controller is designed to maintain the asymptotic stability and robust performance of T-S aero-engine networked system by using Lyapunov function method and switched system theory. Finally, a TrueTime simulation example demonstrates the efficiency of the proposed method. The research provides some theory reference for nonlinear control of aero-engine wireless networked system with signal scheduling under different flight environments, aggressive interference and low-bandwidth conditions

II. T-S NONLINEAR MODEL FOR AERO-ENGINE NETWORKED CONTROL SYSTEMS

System description were provided in the previous literature [18], and based on TOD scheduling strategy [18]–[20], the four factors include η = network bandwidth, θ_k = non-real-time data width, T = sampling period and P = data-packet capacity are defined. In order to include parameter T, P into aero-engine discrete state-space model, relationship between T, P and network delay τ should be obtained firstly. If network is schedulable and data-packet have no passive dropout, the expression at sampling time k is workable as follows.

$$(k+1)\,\bar{P} + \bar{\theta}_k = (kT + \tau(k))\,\eta \tag{1}$$

where $\bar{P} = \iota P$, ι is data width which every transmission variable occupies. $\bar{\theta}_k = \sum_{i=0}^{k} \theta_i$, so the network delay can be obtained by Eq.(1) as follows.

$$\tau(k) = \frac{(k+1)\,\bar{P} + \bar{\theta}_k}{\eta} - kT \tag{2}$$

Let $\tau(k) \in [-T/2, T/2]$, When ignore the noise, the continuous state space model could be expressed as

$$\begin{cases} \dot{x}(t) = A_c x(t) + B_c u(t) + Rd(t) \\ y(t) = C_c x(t) + D_c u(t) \end{cases} \tag{3}$$

where $x(t) \in R^n$ is state variable, $u(t) \in R^m$ is control variable, $d(t)$ is disturbance term.

According to the assumptions, Eq.(4) could be obtained by discretizing the continuous state space model.

$$\begin{aligned} x(k+1) &= Ax(k) + (B_0 + DF_kE)\,v(k) \\ &\quad + (B_1 - DF_kE)\,v(k-1) + Rd(k) \end{aligned} \tag{4}$$

$$A = e^{A_cT},\ B_0 = \int_0^{T/2} e^{A_cs}ds \cdot B,\ B_1 = \int_{T/2}^{T} e^{A_cs}ds \cdot B$$

$$D = \beta e^{A_c(T/2)},\ F_k = \beta^{-1}\int_0^{-\tau(k)} e^{A_cs}ds,\ E = B$$

Here, $\omega(k)$, $v(k)$ are state variable and control variable after active scheduling, which can be expressed as $\omega(k) = \Gamma_\sigma(k)\,x(k) + (I - \Gamma_\sigma(k))\,\omega(k-1)$, $v(k) = \Delta_\sigma(k)\,u(k) + (I - \Delta_\sigma(k))\,v(k-1)$, where $\Gamma_\sigma(k)$ and $\Delta_\sigma(k)$ are scheduling matrixes of system state variable and control variable at sampling time k.

Set $\beta = \max_{\tau(k)} \left\| \int_0^{-\tau(k)} e^{\mathbf{A}_c s} ds \right\|_2 = \left\| \int_0^{T/2} e^{\mathbf{A}_c s} ds \right\|_2$, $F_k^T F_k \leq I$, so Eq.(5) can be obtained by Eq.(4) as follows.

$$x(k+1) = Ax(k) + (B_0 + \beta H F_k E) v(k) + (B_1 - \beta H F_k E) v(k-1) \quad (5)$$

where $H = e^{A_c(T/2)}$. According to the assumption of system with parametric certainties, the problem of design an controller $v(k) = K_\sigma \omega(k)$ based on state feedback is employed, where $K_\sigma \in R^{m \times n}$ is the controller gain matrix, then a joint design method with network and control parameters in consideration for aero-engine networked control systems is obtained by Eq.(5) as follows.

$$\begin{cases} x(k+1) = Ax(k) + (B_0 + \beta H F_k E) v(k) \\ \quad + (B_1 - \beta H F_k E) v(k-1) + Rd(k) \\ \omega(k) = \Gamma_\sigma(k) x(k) + (I - \Gamma_\sigma(k)) \omega(k-1) \\ v(k) = \Delta_\sigma(k) u(k) + (I - \Delta_\sigma(k)) v(k-1) \\ u(k) = K_\sigma \omega(k) \end{cases} \quad (6)$$

When $M_0 = B_0 + \beta H F_k E$, $M_1 = B_1 - \beta H F_k E$, a class of aero-engine T-S fuzzy model based on flight envelop division can be expressed by

R^i: if H_f is Ψ_{1i} and Ma is Ψ_{2i} then

$$\begin{cases} x(k+1) = \left(A_i + M_{0i} \Delta_\sigma K_{\sigma j} \Gamma_\sigma\right) x(k) \\ + \left(M_{0i} \Delta_\sigma K_{\sigma j} (I - \Gamma_\sigma)\right) \omega(k-1) \\ + (M_{0i}(I - \Delta_\sigma) + M_{1i}) v(k-1) + Rd(k) \\ \omega(k) = \Gamma_\sigma(k) x(k) + (I - \Gamma_\sigma(k)) \omega(k-1) \\ v(k) = \Delta_\sigma K_{\sigma j} \Gamma_\sigma x(k) + \Delta_\sigma K_{\sigma j} (I - \Gamma_\sigma) \omega(k-1) \\ + (I - \Delta_\sigma) v(k-1) \end{cases} \quad (7)$$

where R^i is i-th fuzzy rule; H_f is flight height and Ma is Mach number; Ψ_{1i} and Ψ_{2i} are the corresponding fuzzy sets of H_f and Ma. On the basis, the global fuzzy model for any working point in the flight envelop can be obtained as follows.

$$\begin{cases} x(k+1) = \sum_{i=1}^{\theta} \sum_{j=1}^{\theta} \mu_i \mu_j [(A_i + M_{0i} \Delta_\sigma K_{\sigma j} \Gamma_\sigma) x(k) \\ + (M_{0i} \Delta_\sigma K_{\sigma j} (I - \Gamma_\sigma)) \omega(k-1) \\ + (M_{0i}(I - \Delta_\sigma) + M_{1i}) v(k-1)] + \sum_{i=1}^{\theta} R_i d(k) \\ \omega(k) = \Gamma_\sigma(k) x(k) + (I - \Gamma_\sigma(k)) \omega(k-1) \\ v(k) = \sum_{j=1}^{\theta} \mu_j [\Delta_\sigma K_{\sigma j} \Gamma_\sigma x(k) \\ + \Delta_\sigma K_{\sigma j} (I - \Gamma_\sigma) \omega(k-1)] + (I - \Delta_\sigma) v(k-1) \end{cases} \quad (8)$$

where $\mu_i = \omega_i / \sum_{i=1}^{r} \omega_i$ is the membership function value after normalization, $\omega_i = \vartheta_{\psi_{1i}} \cdot \vartheta_{\psi_{2i}}$. $\vartheta_{\psi_{mi}}$ $(m = 1, 2)$ is the membership function value in the fuzzy set ψ_{mi} under the antecedent flight condition of the Eq.(7). From the definition, $\omega_i \geq 0$, $\mu_i \geq 0$, $\sum_{i=1}^{r} \mu_i = 1$.

III. EMBEDDED DESIGN OF OPTIMAL T-S H-INFINITY CONTROLLER WITH SCHEDULING

As aero-engine networked control systems include bus network, Quality of Service (QoS) conflicts with Quality of Performance (QoP). Better QoP requires higher sampling frequency and lossless transmission for state and control variables in every sampling period. However, with the bandwidth limitation of bus network, it is impossible to increase sampling frequency and data packet capacity without limit. Thus, T and P will be the undetermined parameters in the controller design, and

Lemma 1: When a matrix $S = \begin{bmatrix} S_{11} & S_{12} \\ S_{12}^T & S_{22} \end{bmatrix}$, where S_{11}, S_{22} are square matrices, then the following three conditions are equivalent:

(1) $S < 0$;
(2) $S_{22} < 0$, $S_{11} - S_{12} S_{22}^{-1} S_{12}^T < 0$;
(3) $S_{11} < 0$, $S_{22} - S_{12}^T S_{11}^{-1} S_{12} < 0$.

Lemma 2: Given constant matrices $W = W^T, M, N$, for any $F(k)$ subject to $F(k)^T F(k) \leq I$, $W + N^T F(k)^T M^T + M F(k) N < 0$ holds if there is a constant scalar $\varepsilon > 0$ satisfying $W + \varepsilon^{-1} N^T N + \varepsilon M M^T < 0$.

Lemma 3: For any proper dimension of matrices U_{ij}, V_{pq}, $(1 \leq i, j, p, q \leq r)$ and symmetric positive definite matrix T, the following is satisfied:

$$2 \sum_{i=1}^{r} \sum_{j=1}^{r} \sum_{p=1}^{r} \sum_{q=1}^{r} \mu_i \mu_j \mu_p \mu_q \left(U_{ij}^T T V_{pq}\right) \leq \sum_{i=1}^{r} \sum_{j=1}^{r} \mu_i \mu_j \left(U_{ij}^T T U_{ij} + V_{ij}^T T V_{ij}\right)$$

Definition 1: The global fuzzy system (8) is asymptotic stable with H_∞ norm bound γ satisfied if there has a state feedback controller

$$u(k) = \sum_{l=1}^{\theta} \mu_l K_{ml} x(k) \begin{cases} R^l : \text{if } H_f \text{ is } \Psi_{1l} \text{ and } Ma \text{ is } \Psi_{2l} \\ \text{then } K_{mi} \\ (m = 1, 2; i = 1, 2, \cdots, \theta), \end{cases}$$

which is the controller gain under i-th fuzzy rule), and the following conditions are satisfied: (a) The global fuzzy system is asymptotic stable; (b) On the zero-initial condition, for bounded external disturbance $d(k)$ which satisfies $\|y(k)\|_2 < \gamma \|d(k)\|_2$.

Theorem 1: For $\forall i, j \in \{1, 2, \cdots, \theta\}$, $j > i$, and $\forall \sigma \in \{1, 2, \cdots, N\}$ ($1 - N$ represent data transport patterns), if there exist common positive definite matrices W, Q, S, scalars $\varepsilon_1 > 0$, $\varepsilon_{2i} > 0$, $\varepsilon_{2j} > 0$, and $\gamma > 0$ such that inequality (9), (10), as shown at the top of the next page, hold, the global fuzzy system (8) is asymptotic stable with the H_∞ norm bound γ.

Where $\bar{W} = W^{-1}$, $\bar{Q} = Q^{-1}$, $\bar{S} = S^{-1}$, '$*$' denote the entries of matrices implied by symmetry.

Proof: Choosing the Lyapunov functional as

$$V(k) = x(k)^T W x(k) + \omega(k-1)^T Q \omega(k-1) + v(k-1)^T S v(k-1), \text{ then}$$

$$\begin{bmatrix}
-\bar{W} & * & * & * & * & * & * & * & * & * & * \\
0 & -\bar{Q} & * & * & * & * & * & * & * & * & * \\
0 & 0 & -\bar{S} & * & * & * & * & * & * & * & * \\
0 & 0 & 0 & -\gamma^2 I & * & * & * & * & * & * & * \\
A_i\bar{W} & 0 & B_{0i}\bar{S}+B_{1i}\bar{S}-B_{0i}\Delta_\sigma\bar{S} & \Lambda_{\sum} & -\bar{W}+\varepsilon_1\beta_i H_i\,(\beta_i H_i)^T & * & * & * & * & * & * \\
0 & 0 & 0 & 0 & 0 & -\bar{Q} & * & * & * & * & * \\
0 & 0 & \bar{S}-\Delta_\sigma\bar{S} & 0 & 0 & 0 & -\bar{S} & * & * & * & * \\
\bar{W} & 0 & 0 & 0 & 0 & 0 & 0 & -I & * & * & * \\
0 & 0 & -E_i\Delta_\sigma\bar{S} & 0 & 0 & 0 & 0 & 0 & -\varepsilon_1 I & * & * \\
0 & 0 & 0 & 0 & [B_{0i}\Delta_\sigma K_{\sigma i}]^T & I & [\Delta_\sigma K_{\sigma i}]^T & 0 & [E_i\Delta_\sigma K_{\sigma i}]^T & -I & * \\
\Gamma_\sigma\bar{W} & \bar{Q}-\Gamma_\sigma\bar{Q} & 0 & 0 & 0 & 0 & 0 & 0 & 0 & 0 & -I
\end{bmatrix} < 0 \tag{9}$$

$$\begin{bmatrix}
-\bar{W} & * & * & * & * & * & * & * & * & * & * \\
0 & -\bar{Q} & * & * & * & * & * & * & * & * & * \\
0 & 0 & -\bar{S} & * & * & * & * & * & * & * & * \\
0 & 0 & 0 & -\gamma^2 I & * & * & * & * & * & * & * \\
\frac{1}{2}(A_i+A_j)\bar{W} & 0 & \frac{1}{2}(B_{0i}+B_{1i}-B_{0i}\Delta_\sigma+B_{0j}+B_{1j}-B_{0j}\Delta_\sigma)\bar{S} & \Lambda_{\sum} & -\bar{W}+\frac{1}{2}\varepsilon_{2i}\beta_i H_i(\beta_i H_i)^T+\frac{1}{2}\varepsilon_{2j}\beta_j H_j(\beta_j H_j)^T & * & * & * & * & * & * \\
0 & 0 & 0 & 0 & 0 & -\bar{Q} & * & * & * & * & * \\
0 & 0 & \bar{S}-\Delta_\sigma\bar{S} & 0 & 0 & 0 & -\bar{S} & * & * & * & * \\
\bar{W} & 0 & 0 & 0 & 0 & 0 & 0 & -I & * & * & * \\
0 & 0 & -E_i\Delta_\sigma\bar{S} & 0 & 0 & 0 & 0 & 0 & -2\varepsilon_{2i}I & * & * \\
0 & 0 & -E_j\Delta_\sigma\bar{S} & 0 & 0 & 0 & 0 & 0 & 0 & -2\varepsilon_{2j}I & * \\
0 & 0 & 0 & 0 & \frac{1}{2}(B_{0i}\Delta_\sigma K_{\sigma j}+B_{0j}\Delta_\sigma K_{\sigma i})^T & I & (\Delta_\sigma K_{\sigma i})^T & 0 & (E_i\Delta_\sigma K_{\sigma j})^T & (E_j\Delta_\sigma K_{\sigma i})^T & -I \\
\Gamma_\sigma\bar{W} & \bar{Q}-\Gamma_\sigma\bar{Q} & 0 & 0 & 0 & 0 & 0 & 0 & 0 & 0 & -I
\end{bmatrix} < 0 \tag{10}$$

$$\begin{aligned}
\Delta V(k) &= V(k+1)-V(k) \\
&= x(k+1)^T Wx(k+1)+\omega(k)^T Q\omega(k) \\
&\quad +v(k)^T Sv(k)- \\
&\quad x(k)^T Wx(k)-\omega(k-1)^T Q\omega(k-1) \\
&\quad -v(k-1)^T Sv(k-1)
\end{aligned}$$

For easy deduction, the following definitions are given:

$$\begin{aligned}
G_{1\sigma} &= A+M_0\Delta_\sigma K_\sigma\Gamma_\sigma, G_{2\sigma}=M_0\Delta_\sigma K_\sigma(I-\Gamma_\sigma), \\
G_{3\sigma} &= M_0(I-\Delta_\sigma)+M_1, U_{1\sigma}=\Delta_\sigma K_\sigma\Gamma_\sigma, \\
U_{2\sigma} &= \Delta_\sigma K_\sigma(I-\Gamma_\sigma)z(k) \\
&= \left[x(k)^T\ \omega(k-1)^T\ v(k-1)^T\ d(k)^T\right]^T,
\end{aligned}$$

then $\Delta V(k)$ is given in the equation shown at the top of the next page.

According to Lemma 3, the equation shown at the top of the next page is given.

Let $\Lambda_\Sigma = \sum_{i=1}^{\theta}\bar{R}_i$, $\Phi_{ij} = \left[G_{1\sigma ij}\ G_{2\sigma ij}\ G_{3\sigma ij}\ \Lambda_\Sigma\right]$, $\Theta_{ij} = \left[U_{1\sigma i}\ U_{2\sigma i}\ I-\Delta_\sigma\ 0\right]$, then $\Delta V(k)$ is given in the equation shown at the top of the next page.

Considering $0<\mu_i<1, (i=1,2,\cdots,\theta)$, when (11) and (12) hold, as shown at the bottom of page 6, if $d(k)\equiv 0$, $\Delta V(k)<0$, so the system (8) is asymptotic stable; else if $d(k)\neq 0$, $x(k)^T x(k)-\gamma^2 d(k)^T d(k)<-\Delta V(k)$, so under the zero-initial condition,

$$\sum_{k=0}^{\infty} x(k)^T x(k)-\gamma^2\sum_{k=0}^{\infty} d(k)^T d(k)<-V(\infty)<0,$$

that is $\sum_{k=0}^{\infty} x(k)^T x(k)<\gamma^2\sum_{k=0}^{\infty} d(k)^T d(k)$.

From the stability analysis above, it needs to satisfy inequalities (11), (12) to maintain the closed-loop system asymptotic stability with H_∞ performance based on T-S fuzzy flight envelop model.

By Lemma 1,2, inequalities (11), (12) are equivalent to inequalities (13), (14), as shown at the bottom of page 6, where

$$\begin{aligned}
\mathrm{X}_{ij} &= \frac{1}{2}\left(A_i+B_{0i}\Delta_\sigma K_{\sigma j}\Gamma_\sigma+A_j+B_{0j}\Delta_\sigma K_{\sigma i}\Gamma_\sigma\right), \\
\mathrm{X}_{2ij} &= \frac{1}{2}\left(B_{0i}\Delta_\sigma K_{\sigma j}(I-\Gamma_\sigma)+B_{0j}\Delta_\sigma K_{\sigma i}(I-\Gamma_\sigma)\right), \\
\mathrm{X}_{3ij} &= \frac{1}{2}\left(B_{0i}+B_{1i}-B_{0i}\Delta_\sigma+B_{0j}+B_{1j}-B_{0j}\Delta_\sigma\right),
\end{aligned}$$

then according to Lemma 1,2 again, and pre-multiplying and post-multiplying (13), (14) by

$$diag\left(W^{-1},Q^{-1},S^{-1},\overbrace{I,I,I,I,I,I,I}^{6or7}\right)$$

yield (9), (10). The proof is completed.

IV. SIMULATION AND RESULT ANALYSIS

A. AERO-ENGINE T-S NONLINEAR MODEL

200 normalized data (120 for training and 80 for checking) from AL-31F aero-engine is input into the T-S fuzzy nonlinear model which is adaptively optimized by Artificial Neural Network (ANN), and the initial membership function is shown in Fig.1. Then the final membership functions (Fig.2, 3), training results (Fig.4), checking (predicting) results (Fig.5), and errors (Fig.6) are obtained. According to

$$\Delta V(k) = z(k)^T \left\{ \sum_{i=1}^{\theta}\sum_{j=1}^{\theta}\sum_{p=1}^{\theta}\sum_{q=1}^{\theta} \mu_i\mu_j\mu_p\mu_q \begin{bmatrix} G_{1\sigma ij}^T \\ G_{2\sigma ij}^T \\ G_{3\sigma i}^T \\ 0 \end{bmatrix} W \begin{bmatrix} G_{1\sigma pq}^T \\ G_{2\sigma pq}^T \\ G_{3\sigma p}^T \\ 0 \end{bmatrix}^T + \begin{bmatrix} \Gamma_\sigma^T \\ (I-\Gamma_\sigma)^T \\ 0 \\ 0 \end{bmatrix} Q \begin{bmatrix} \Gamma_\sigma^T \\ (I-\Gamma_\sigma)^T \\ 0 \\ 0 \end{bmatrix}^T \right.$$
$$+ \sum_{j=1}^{\theta}\sum_{q=1}^{\theta} \mu_j\mu_q \begin{bmatrix} U_{1\sigma j}^T \\ U_{2\sigma j}^T \\ (I-\Delta_\sigma)^T \\ 0 \end{bmatrix} S \begin{bmatrix} U_{1\sigma q}^T \\ U_{2\sigma q}^T \\ (I-\Delta_\sigma)^T \\ 0 \end{bmatrix}^T + \left. \begin{bmatrix} I-W & 0 & 0 & 0 \\ 0 & -Q & 0 & 0 \\ 0 & 0 & -S & 0 \\ 0 & 0 & 0 & -\gamma^2 I \end{bmatrix} \right\} z(k) + \sum_{i=1}^{\theta}\sum_{p=1}^{\theta}\sum_{q=1}^{\theta} \mu_i\mu_p\mu_q$$
$$\times \begin{bmatrix} 2d(k)^T R_i^T W \left(A_p + M_{0p}\Delta_\sigma K_{\sigma q}\Gamma_\sigma\right) x(k) + 2d(k)^T R_i^T W \left(M_{0p}\Delta_\sigma K_{\sigma q}(I-\Gamma_\sigma)\right)\omega(k-1) \\ +2d(k)^T R_i^T W \left(M_{0p}(I-\Delta_\sigma) + M_{1p}\right) v(k-1) + d(k)^T R_i^T W R_i d(k) \end{bmatrix}$$
$$- \left[x(k)^T x(k) - \gamma^2 d(k)^T d(k) \right]$$

$$\sum_{i=1}^{\theta}\sum_{j=1}^{\theta}\sum_{p=1}^{\theta}\sum_{q=1}^{\theta} \mu_i\mu_j\mu_p\mu_q \begin{bmatrix} G_{1\sigma ij}^T \\ G_{2\sigma ij}^T \\ G_{3\sigma i}^T \\ 0 \end{bmatrix} W \begin{bmatrix} G_{1\sigma pq}^T \\ G_{2\sigma pq}^T \\ G_{3\sigma p}^T \\ 0 \end{bmatrix}^T \le \sum_{i=1}^{\theta}\sum_{j=1}^{\theta} \mu_i\mu_j \begin{bmatrix} G_{1\sigma ij}^T \\ G_{2\sigma ij}^T \\ G_{3\sigma i}^T \\ 0 \end{bmatrix} W \begin{bmatrix} G_{1\sigma ij}^T \\ G_{2\sigma ij}^T \\ G_{3\sigma i}^T \\ 0 \end{bmatrix}^T,$$
$$\sum_{j=1}^{\theta}\sum_{q=1}^{\theta} \mu_j\mu_q \begin{bmatrix} U_{1\sigma j}^T \\ U_{2\sigma j}^T \\ (I-\Delta_\sigma)^T \\ 0 \end{bmatrix} S \begin{bmatrix} U_{1\sigma q}^T \\ U_{2\sigma q}^T \\ (I-\Delta_\sigma)^T \\ 0 \end{bmatrix}^T \le \sum_{j=1}^{\theta} \mu_j \begin{bmatrix} U_{1\sigma j}^T \\ U_{2\sigma j}^T \\ (I-\Delta_\sigma)^T \\ 0 \end{bmatrix} S \begin{bmatrix} U_{1\sigma j}^T \\ U_{2\sigma j}^T \\ (I-\Delta_\sigma)^T \\ 0 \end{bmatrix}^T$$

$$\Delta V(k) \le \sum_{i=1}^{\theta} \mu_i z(k)^T \left\{ \Phi_{ii}^T W \Phi_{ii} + \Theta_i^T S \Theta_i + \begin{bmatrix} \Gamma_\sigma^T \\ (I-\Gamma_\sigma)^T \\ 0 \\ 0 \end{bmatrix} Q \begin{bmatrix} \Gamma_\sigma^T \\ (I-\Gamma_\sigma)^T \\ 0 \\ 0 \end{bmatrix}^T + \begin{bmatrix} -W & 0 & 0 & 0 \\ 0 & -Q & 0 & 0 \\ 0 & 0 & -S & 0 \\ 0 & 0 & 0 & -\gamma^2 I \end{bmatrix} \right.$$
$$\left. + \begin{bmatrix} I & 0 & 0 & 0 \end{bmatrix}^T \begin{bmatrix} I & 0 & 0 & 0 \end{bmatrix} \right\} z(k) + 2\sum_{i=1}^{\theta}\sum_{j=i+1}^{\theta} \mu_i\mu_j z(k)^T \left\{ \left(\frac{\Phi_{ij}+\Phi_{ji}}{2}\right)^T W \left(\frac{\Phi_{ij}+\Phi_{ji}}{2}\right) + \Theta_j^T S \Theta_j \right.$$
$$+ \begin{bmatrix} \Gamma_\sigma^T \\ (I-\Gamma_\sigma)^T \\ 0 \\ 0 \end{bmatrix} Q \begin{bmatrix} \Gamma_\sigma^T \\ (I-\Gamma_\sigma)^T \\ 0 \\ 0 \end{bmatrix}^T + \begin{bmatrix} -W & 0 & 0 & 0 \\ 0 & -Q & 0 & 0 \\ 0 & 0 & -S & 0 \\ 0 & 0 & 0 & -\gamma^2 I \end{bmatrix}$$
$$\left. + \begin{bmatrix} I & 0 & 0 & 0 \end{bmatrix}^T \begin{bmatrix} I & 0 & 0 & 0 \end{bmatrix} \right\} z(k) - x(k)^T x(k) + \gamma^2 d(k)^T d(k)$$

---

the final membership functions, the four optimal T-S fuzzy rules with the selections of H_f and Ma are organized as follows, and the small deviation state space parameters are obtained by aero-engine NCS semi-physical platform under each fuzzy rule.

R^1 : if H_f is about 0.00km and $Ma$is about 0.11 then

$$A_1 = \begin{bmatrix} -1.26364 & 1.0361 \\ -0.15054 & -1.24944 \end{bmatrix}, B_1 = \begin{bmatrix} 0.3542 & 0.54739 \\ 0.35765 & 0.32159 \end{bmatrix},$$
$$R_1 = \begin{bmatrix} 0.0468 \\ 0.0283 \end{bmatrix}$$

R^2 : if H_f is about 6.86km and Ma is about 0.75 then

$$A_2 = \begin{bmatrix} -0.68796 & 0.56623 \\ -0.10917 & -0.74529 \end{bmatrix}, B_2 = \begin{bmatrix} 0.23334 & 0.32494 \\ 0.21948 & 0.21712 \end{bmatrix},$$
$$R_2 = \begin{bmatrix} 0.0359 \\ 0.0153 \end{bmatrix}$$

R^3 : if H_f is about 16.27 km and Ma is about 1.44 then

$$A_3 = \begin{bmatrix} -0.70638 & 0.33246 \\ -0.13549 & -0.37354 \end{bmatrix}, B_3 = \begin{bmatrix} 0.10421 & 0.15536 \\ 0.10228 & 0.08665 \end{bmatrix},$$
$$R_3 = \begin{bmatrix} 0.0225 \\ -0.0147 \end{bmatrix}$$

R^4 : if H_f is about 13.61 km and Ma is about 1.40 then

$$A_4 = \begin{bmatrix} -0.89628 & 0.51077 \\ -0.18259 & -0.56626 \end{bmatrix}, B_4 = \begin{bmatrix} 0.14051 & 0.27368 \\ 0.15398 & 0.13103 \end{bmatrix},$$
$$R_4 = \begin{bmatrix} 0.0055 \\ 0.0078 \end{bmatrix}$$

corresponding to system (8), and $C = \begin{bmatrix} 1 & 0 \\ 0 & 1 \end{bmatrix}$, $x = [n_L, n_H]$, $u = [m_f, A_8]$, where n_L = low-pressure rotor speed; n_H = high-pressure rotor speed; m_f = main chamber fuel delivery; A_8 = nozzle area.

In order to check the model nonlinearity, four random conditions are chosen in the flight envelop, and the membership values are calculated through the final membership functions and shown in Tab.1.

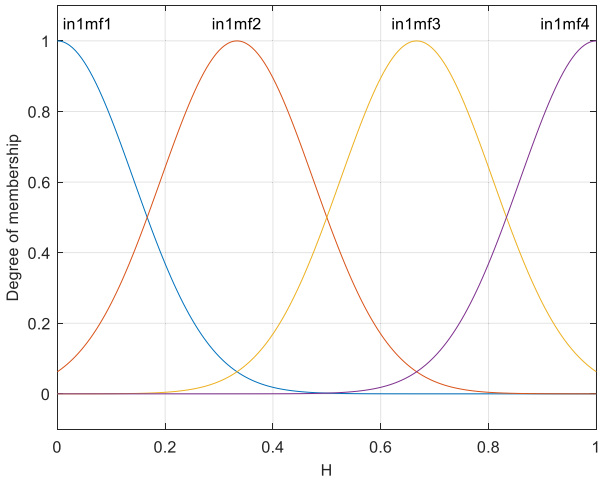

FIGURE 1. Initial membership function.

B. CONTROLLER DESIGN AND RESULT ANALYSIS

To verify the approach, TrueTime simulation platform [18] and the simplified block model of aero-engine wireless networked control is established shown in Fig.7 and Fig.8, in which Nonperiodic interference, Wireless Network, Aero-engine, Intelligent sensor, H-infinity controller, Actuator, TrueTime send and TrueTime receive are included. The nonlinear control method and real time scheduling strategy are coded into the intelligent sensor and controller module.

$$\Phi_{ii}^T W \Phi_{ii} + \Theta_i^T S \Theta_i + \begin{bmatrix} \Gamma_\sigma^T \\ (I-\Gamma_\sigma)^T \\ 0 \\ 0 \end{bmatrix} Q \begin{bmatrix} \Gamma_\sigma^T \\ (I-\Gamma_\sigma)^T \\ 0 \\ 0 \end{bmatrix}^T + \begin{bmatrix} -W & 0 & 0 & 0 \\ 0 & -Q & 0 & 0 \\ 0 & 0 & -S & 0 \\ 0 & 0 & 0 & -\gamma^2 I \end{bmatrix} + \begin{bmatrix} I & 0 & 0 & 0 \end{bmatrix}^T \begin{bmatrix} I & 0 & 0 & 0 \end{bmatrix} < 0 \quad (11)$$

$$\left(\frac{\Phi_{ij}+\Phi_{ji}}{2}\right)^T W \left(\frac{\Phi_{ij}+\Phi_{ji}}{2}\right) + \Theta_j^T S \Theta_j + \begin{bmatrix} \Gamma_\sigma^T \\ (I-\Gamma_\sigma)^T \\ 0 \\ 0 \end{bmatrix} Q \begin{bmatrix} \Gamma_\sigma^T \\ (I-\Gamma_\sigma)^T \\ 0 \\ 0 \end{bmatrix}^T + \begin{bmatrix} -W & 0 & 0 & 0 \\ 0 & -Q & 0 & 0 \\ 0 & 0 & -S & 0 \\ 0 & 0 & 0 & -\gamma^2 I \end{bmatrix}$$
$$+ \begin{bmatrix} I & 0 & 0 & 0 \end{bmatrix}^T \begin{bmatrix} I & 0 & 0 & 0 \end{bmatrix} < 0 \quad (12)$$

$$\begin{bmatrix} -W & * & * & * & * & * & * & * & * \\ 0 & -Q & * & * & * & * & * & * & * \\ 0 & 0 & -S & * & * & * & * & * & * \\ 0 & 0 & 0 & -\gamma^2 I & * & * & * & * & * \\ A_i + B_{0i}\Delta_\sigma K_{\sigma i}\Gamma_\sigma & B_{0i}\Delta_\sigma K_{\sigma j}(I-\Gamma_\sigma) & B_{0i} + B_{1i} - B_{0i}\Delta_\sigma & \Lambda_\sum & -W^{-1} + \varepsilon_1 \beta_i H_i (\beta_i H_i)^T & * & * & * & * \\ \Gamma_\sigma & I - \Gamma_\sigma & 0 & 0 & 0 & -Q^{-1} & * & * & * \\ \Delta_\sigma K_{\sigma i}\Gamma_\sigma & \Delta_\sigma K_{\sigma i}(I-\Gamma_\sigma) & I - \Delta_\sigma & 0 & 0 & 0 & -S^{-1} & * & * \\ I & 0 & 0 & 0 & 0 & 0 & 0 & -I & * \\ E_i\Delta_\sigma K_{\sigma i}\Gamma_\sigma & E_i\Delta_\sigma K_{\sigma i}(I-\Gamma_\sigma) & -E_i\Delta_\sigma & 0 & 0 & 0 & 0 & 0 & -\varepsilon_1 I \end{bmatrix} < 0 \quad (13)$$

$$\begin{bmatrix} -W & * & * & * & * & * & * & * & * & * \\ 0 & -Q & * & * & * & * & * & * & * & * \\ 0 & 0 & -S & * & * & * & * & * & * & * \\ 0 & 0 & 0 & -\gamma^2 I & * & * & * & * & * & * \\ X_{1ij} & X_{2ij} & X_{3ij} & \Lambda_\sum & -W^{-1} + \frac{1}{2}\varepsilon_{2i}\beta_i H_i (\beta_i H_i)^T + \frac{1}{2}\varepsilon_{2j}\beta_j H_j (\beta_j H_j)^T & * & * & * & * & * \\ \Gamma_\sigma & I - \Gamma_\sigma & 0 & 0 & 0 & -Q^{-1} & * & * & * & * \\ \Delta_\sigma K_{\sigma i}\Gamma_\sigma & \Delta_\sigma K_{\sigma i}(I-\Gamma_\sigma) & I - \Delta_\sigma & 0 & 0 & 0 & -S^{-1} & * & * & * \\ I & 0 & 0 & 0 & 0 & 0 & 0 & -I & * & * \\ E_i\Delta_\sigma K_{\sigma j}\Gamma_\sigma & E_i\Delta_\sigma K_{\sigma j}(I-\Gamma_\sigma) & -E_i\Delta_\sigma & 0 & 0 & 0 & 0 & 0 & -2\varepsilon_{2i} I & * \\ E_j\Delta_\sigma K_{\sigma i}\Gamma_\sigma & E_j\Delta_\sigma K_{\sigma i}(I-\Gamma_\sigma) & -E_j\Delta_\sigma & 0 & 0 & 0 & 0 & 0 & 0 & -2\varepsilon_{2j} I \end{bmatrix} < 0 \quad (14)$$

TABLE 1. Membership values in diffierent rules.

Condition	H_f	Ma	μ_1	μ_2	μ_3	μ_4
1	3.98	0.38	0.911398	0.041062	0.047539	0
2	7.97	0.77	0.012510	0.8203496	0.167051	0
3	11.95	1.15	0	0.0002826	0.954091	0.045627
4	15.94	1.54	0	0	0.854587	0.145412

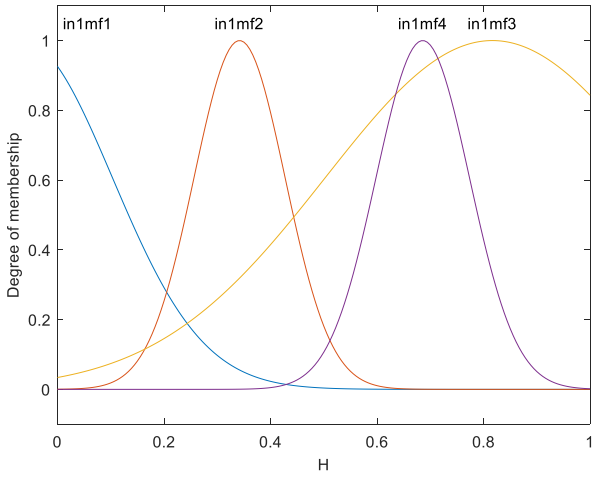

FIGURE 2. Final membership function of H_f.

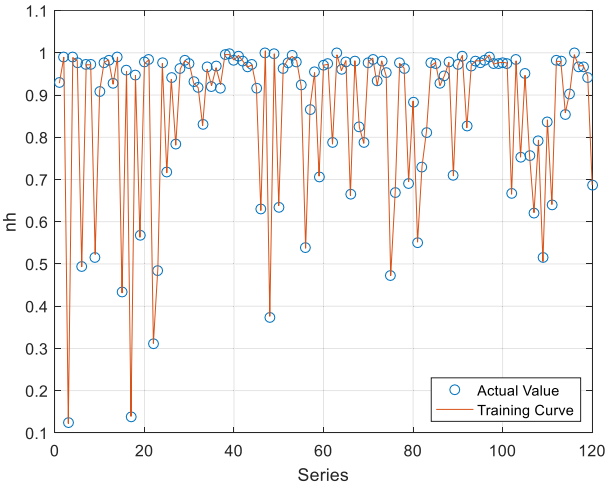

FIGURE 4. Training results.

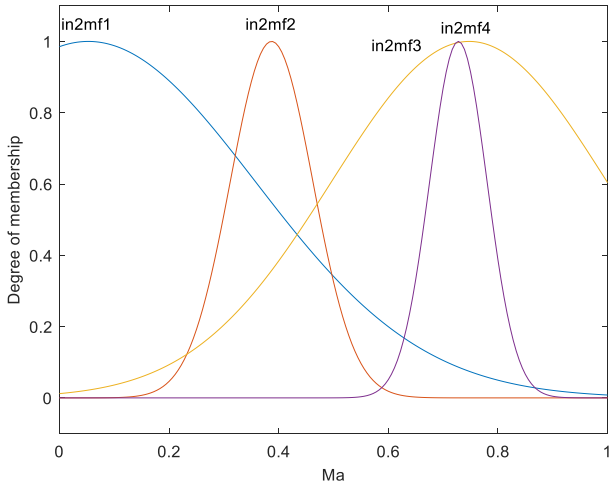

FIGURE 3. Final membership function of *Ma*.

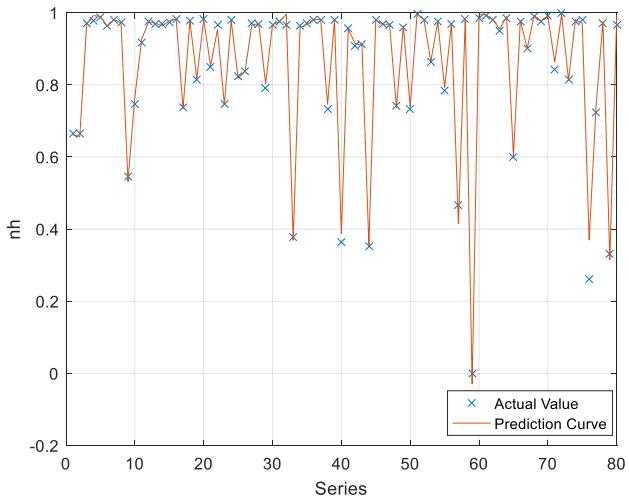

FIGURE 5. Checking results.

The TrueTime Sends were triggered by the fixed waveform, and although the sensor, controller and actuators could communicate with each other in the single channel, the realization of multi-channel by introducing the TrueTime Sends could present the dynamic scheduling more visually. When the signals were limited to transmit, the self-contained single channels would be working to transmit the rest signal of sensor or controller, and the corresponding TrueTime sends would not get and send message even if they were triggered. When the signals were not limited, the TrueTime Send multi-channels would be working to transmit all the sensor or controller signals, and the self-contained single channels would not send message. Through the presented simulation technical method, signal limitation and scheduling could be real-time observed by the service of single channels.

As the relation between real-time bandwidth and physical bandwidth is

$$\theta_k + \iota P \leq T\eta \tag{15}$$

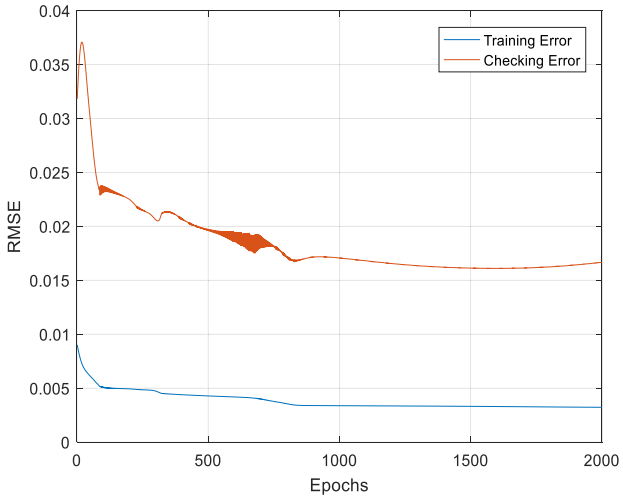

FIGURE 6. Error curves.

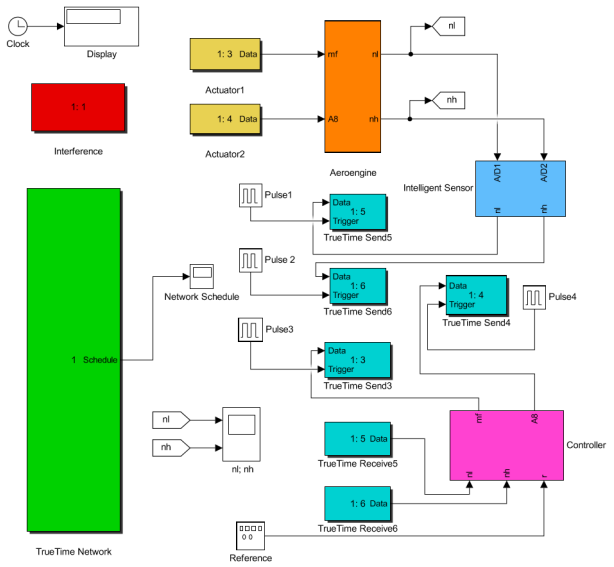

FIGURE 7. TrueTime simulation platform for aero-engine wireless networked control system.

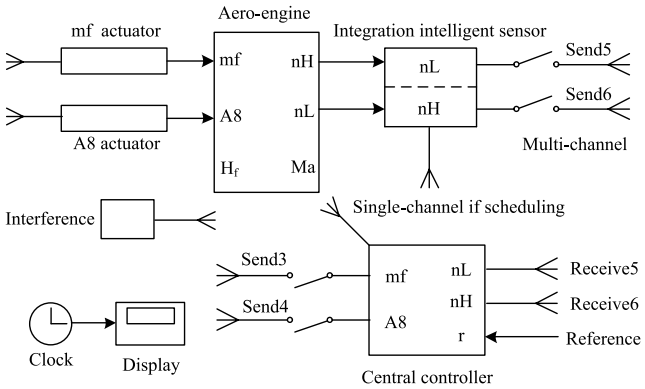

FIGURE 8. Simplified block model of the truetime simulation.

where the parameters are initialed as $T = 0.015$s, $P = 3$, $\eta =$ 30000bit/s, ι=110, $\theta_k = 80$bit, and the interference sending probability $= 20\%$. These network parameters were chosen

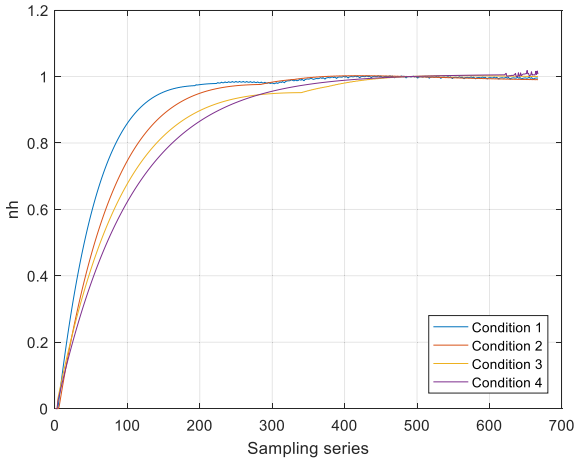

FIGURE 9. System step response results of $T, P = (0.015\text{s}, 3)$.

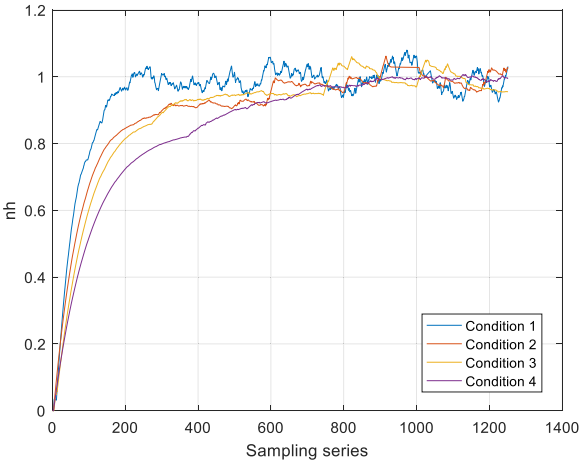

FIGURE 10. System step response results of $T, P = (0.008\text{s}, 2)$.

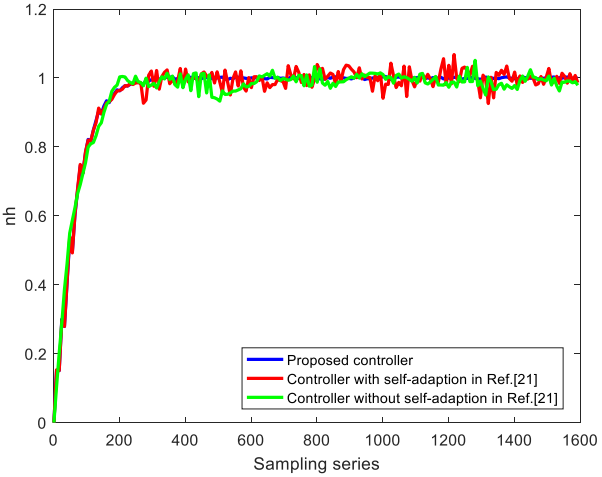

FIGURE 11. Comparison between the proposed controller and controller in reference [21].

by heuristic algorithm, and the variable calculation iterations were about 40 times with the suitable step length. There will be some alternative if the corresponding conditions have the same optimal upper bound, and the best network parameter combination should be picked out according to QoP. Because there are two states and two control input signals

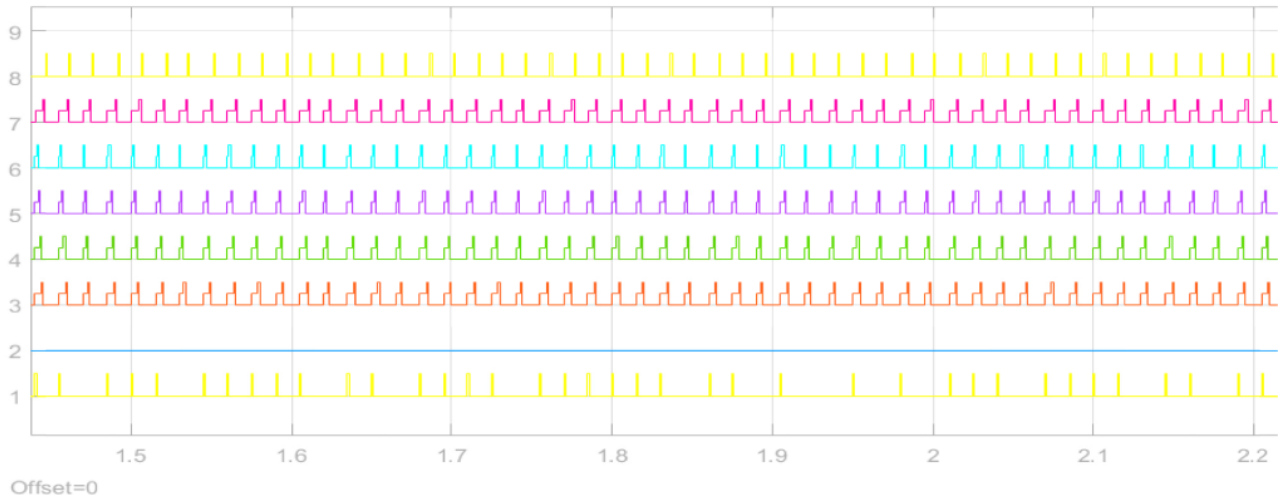

FIGURE 12. Partial scheduling results in the beginning phase.

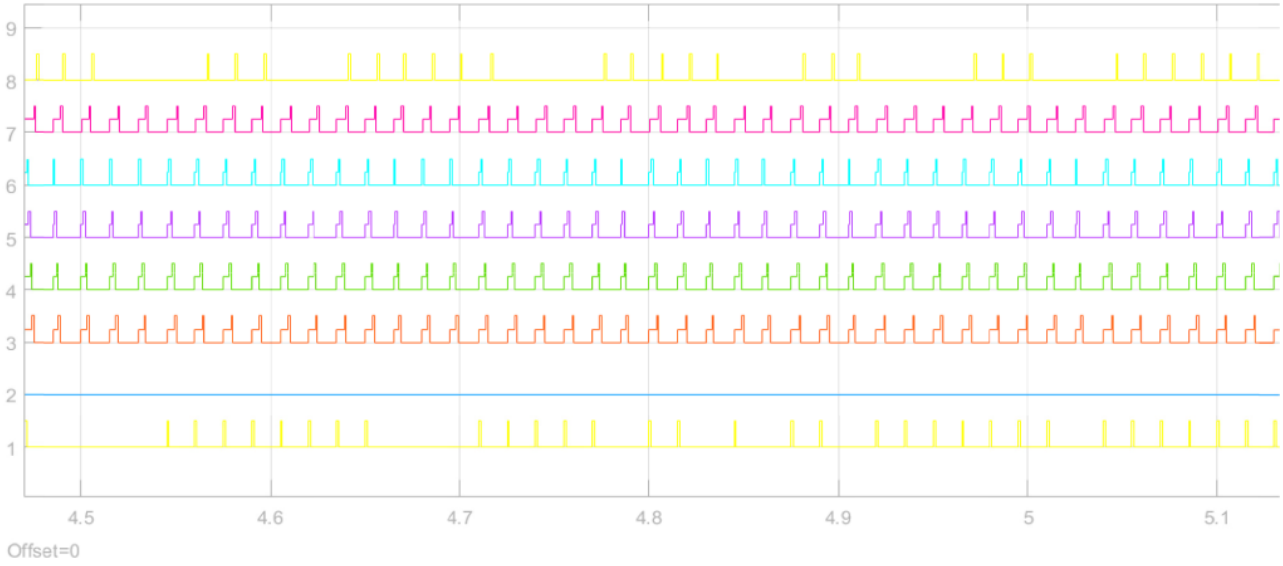

FIGURE 13. Partial scheduling results in the middle phase.

in the system, then the aero-engine networked system has four transmission patterns (σ) under the four conditions (i), by giving $\gamma = 6 - 8$ which is debugged for the best controller performance, and solving the LMIs in Theorem 1, we obtain the controller gains under the four transmission patterns as:

$$\Psi_1 = diag\left(1\ 0\ 1\ 1\right), K_{11} = \begin{bmatrix} 0.176077 & -0.06875 \\ -0.0281 & 0.023174 \end{bmatrix},$$

$$K_{12} = \begin{bmatrix} 0 & 0 \\ 0 & -0.13245 \end{bmatrix},$$

$$K_{13} = \begin{bmatrix} -0.23719 & 0 \\ 0 & 0 \end{bmatrix}, K_{14} = \begin{bmatrix} 0.051692 & -0.06376 \\ -0.04035 & 0.294157 \end{bmatrix}$$

$$\Psi_2 = diag\left(0\ 1\ 1\ 1\right), K_{21} = \begin{bmatrix} 0.366506 & -0.05151 \\ -0.06123 & 0.050522 \end{bmatrix},$$

$$K_{22} = \begin{bmatrix} 0 & 0 \\ 0 & -0.03192 \end{bmatrix},$$

$$K_{23} = \begin{bmatrix} -0.03603 & 0 \\ 0 & 0 \end{bmatrix}, K_{24} = \begin{bmatrix} 0.109275 & -0.13034 \\ -0.08738 & 0.547948 \end{bmatrix}$$

$$\Psi_3 = diag\left(1\ 1\ 0\ 1\right), K_{31} = \begin{bmatrix} 0.549193 & -0.0878 \\ -0.05676 & 0.044557 \end{bmatrix},$$

$$K_{32} = \begin{bmatrix} 0 & 0 \\ 0 & -0.03043 \end{bmatrix},$$

$$K_{33} = \begin{bmatrix} -0.03967 & 0 \\ 0 & 0 \end{bmatrix}, K_{34} = \begin{bmatrix} 0.166031 & -0.16142 \\ -0.12414 & 1.080131 \end{bmatrix}$$

$$\Psi_4 = diag\left(1\ 1\ 1\ 0\right), K_{41} = \begin{bmatrix} 0.535695 & -0.08977 \\ -0.05606 & 0.043963 \end{bmatrix},$$

$$K_{42} = \begin{bmatrix} 0 & 0 \\ 0 & -0.06322 \end{bmatrix},$$
$$K_{43} = \begin{bmatrix} -0.05046 & 0 \\ 0 & 0 \end{bmatrix}, K_{44} = \begin{bmatrix} 0.15523 & -0.15112 \\ -0.11609 & 1.000796 \end{bmatrix}$$

Under the four checking conditions, output step responses are shown in Fig.9. From the figure, asymptotic stability can be ensured, and the better robustness of the nonlinear controller can be indicated. As $P = \{1, 2, 3, 4\}$, if $P = 4$, all of the signals will be transmitted, and the presented scheduling method will not work. If $P = 1$, the QoP will be worse and the state variables are hard to converge. Thus, if $P = 2$, the best $T = 0.008$s which can be calculated through heuristic optimization. For comparing, after changing the two parameter T, $P = (0.008\text{s}, 2)$, the results (in Fig.10) showed the obvious state errors and a degree of decrease for system dynamic performance. Thus, it proved the network influence on control performance in the joint design model.

For comparison, aero-engine T-S fuzzy sliding mode controller based on flight envelop division proposed in our previous research [21] is employed. Although the sliding mode controller is not embedded with scheduling algorithm, it has the advantage of anti-interference and self-adaption performance. Under the above network condition of $T = 0.015$s, $P = 3$, and the interference sending probability $= 20\%$, system state response curves are shown in Fig.11. According to the result, the TOD embedded T-S H-infinity controller has better QoP in the circumstance of data-packet transmission restraints, and the self-adaption of the T-S sliding mode controller cannot reduce the chattering caused by controller or actuator data missing. Thus, the effectiveness of the proposed approach has been verified.

Partial scheduling results is shown in Fig.12,13, and from bottom to top, they are disturbance signal (1), signal reserved for H_f and Ma in the future research (2), TrueTime send3 (3), TrueTime send4 (4), TrueTime send5 (5), TrueTime send6 (6), scheduling signal (7), single controller signal (8). For each curve, low situation means 'unsent', middle situation means 'waiting to send', high situation means 'sending'. After the system tends to be stable in the middle phase (Fig.13), the curve (8) shows that the controller begins to send all of the two control signals with the help of TrueTime send3 (3) and TrueTime send4 (4), which means the state errors may be less enough for the system to limit the two state signals rather than the two control signals.

V. CONCLUSION

In this paper, the traditional time-invariant aero-engine networked control system was extended to the full flight envelop nonlinear systems with active signal scheduling. Wireless simulation switching technique of single-channel and multi-channel was adopted to verify the QoP under the interference and intelligent scheduling network. Dynamic signal scheduling and H-infinity stabilization for a class of nonlinear aero-engine wireless networked control systems with external disturbances has been investigated. The adaptive T-S fuzzy system is modeled based on flight envelop division, then a co-design method of MEF-TOD dynamic scheduling strategy and the robust H-infinity controller is developed to guarantee the asymptotic stability and good robust performance of the closed-loop aero-engine networked control systems. Under four random conditions, simulation with real aero-engine data has been given to demonstrate the effectiveness of the proposed scheme.

CONFLICTS OF INTEREST

The authors declare that they have no conflicts of interest.

REFERENCES

[1] Y. Pan and G.-H. Yang, "Event-based reduced-order fuzzy filtering for networked control systems with time-varying delays," *Appl. Math. Comput.*, vol. 359, pp. 71–83, Oct. 2019.

[2] X. L. Chen, Y. G. Wang, and S. L. Hu, "Event-triggered quantized H_∞ control for networked control systems in the presence of denial-of-service jamming attacks," *Nonlinear Anal., Hybrid Syst.*, vol. 33, pp. 265–281, Aug. 2019.

[3] S. Linsenmayer, D. V. Dimarogonas, and F. Allgöwer, "Periodic event-triggered control for networked control systems based on non-monotonic Lyapunov functions," *Automatica*, vol. 106, pp. 35–46, Aug. 2019.

[4] X. Chu and M. Li, "Observer-based model following sliding mode tracking control of discrete-time linear networked systems with two-channel event-triggered schemes and quantizations," *Appl. Math. Comput.*, vol. 355, pp. 428–448, Aug. 2019.

[5] S. Xiong, M. Chen, and Q. Wu, "Predictive control for networked switch flight system with packet dropout," *Appl. Math. Comput.*, vol. 354, pp. 444–459, Aug. 2019.

[6] T. Li, X. Tang, H. Zhang, and S. Fei, "Improved event-triggered control for networked control systems under stochastic cyber-attacks," *Neurocomputing*, vol. 350, pp. 33–43, Jul. 2019.

[7] Y. Guan and C. Peng, "A hybrid transmission scheme for networked control systems," *ISA Trans.*, to be published.

[8] H.-Y. Chu, S.-M. Fei, H.-X. Chen, and J.-Y. Zhai, "T-S-fuzzy-model-based quantized control for nonlinear networked control systems," *J. Southeast Univ., English Ed.*, vol. 26, no. 1, pp. 137–141, 2010.

[9] M. O. T. Cole, C. Chamroon, and P. S. Keogh, "H-infinity controller design for active magnetic bearings considering nonlinear vibrational rotordynamics," *Mech. Eng. J.*, vol. 4, no. 5, p. 716, 2017.

[10] M. E. Elhaji and C. J. Hatziadoniu, "Interarea oscillation damping using H-infinity control for the permanent magnet wind generator," *Electr. Power Syst. Res.*, vol. 151, pp. 319–328, Oct. 2017.

[11] C. A. X. da Silva, D. A. Colombo, R. F. Corrêa, F. A. Lara-Molina, and E. H. Koroishi, "Active vibration control applying H-infinity norm in a composite laminated beam," in *Transdisciplinary Engineering: Crossing Boundaries* (Advances in Transdisciplinary Engineering), vol. 4. 2016, pp. 461–470.

[12] Y. Wang, H. Shen, H. R. Karimi, and D. Duan, "Dissipativity-based fuzzy integral sliding mode control of continuous-time T-S fuzzy systems," *IEEE Trans. Fuzzy Syst.*, vol. 26, no. 3, pp. 1164–1176, Jun. 2018.

[13] J. Dong and G.-H. Yang, "Observer-based output feedback control for discrete-time T-S fuzzy systems with partly immeasurable premise variables," *IEEE Trans. Syst., Man, Cybern., Syst.*, vol. 47, no. 1, pp. 98–110, Jan. 2017.

[14] D. Liu, G.-H. Yang, and M. J. Er, "Event-triggered control for T-S fuzzy systems under asynchronous network communications," *IEEE Trans. Fuzzy Syst.*, to be published. doi: 10.1109/TFUZZ.2019.2906857.

[15] H. Zhang, P. Cheng, L. Shi, and J. Chen, "Optimal DoS attack scheduling in wireless networked control system," *IEEE Trans. Control Syst. Technol.*, vol. 24, no. 3, pp. 843–852, May 2016.

[16] X. Wang, Z. Li, and W. Wonham, "Dynamic multiple-period reconfiguration of real-time scheduling based on timed DES supervisory control," *IEEE Trans. Ind. Informat.*, vol. 12, no. 1, pp. 101–111, Feb. 2016.

[17] H.-J. Cha, W.-H. Jeong, and J.-C. Kim, "Control-scheduling codesign exploiting trade-off between task periods and deadlines," *Mobile Inf. Syst.*, vol. 2016, Mar. 2016, Art. no. 3414816.

[18] B. Zhou, S. Xie, L. Wang, Y. Zhang, L. Zhang, H. Wang, and L. Ren, "Piecewise adaptive sliding mode control for aeroengine networked control systems with resource constraints," *Complexity*, vol. 2019, Feb. 2019, Art. no. 8693780.
[19] C. Zhou, M. Du, and Q. Chen, "Co-design of dynamic scheduling and H-infinity control for networked control systems," *Appl. Math. Comput.*, vol. 218, pp. 10767–10775, Jul. 2012.
[20] C. Zhou, H. Lu, J. Ren, and Q. W. Chen, "Co-design of dynamic scheduling and quantized control for networked control systems," *J. Franklin Inst.*, vol. 352, no. 10, pp. 3988–4003, Oct. 2015.
[21] L. T. Ren, S. S. Xie, and J. B. Peng, "Adaptive robust sliding mode control for aeroengine T-S distributed system," *J. Propuls. Technol.*, vol. 37, no. 12, pp. 2366–2376, 2016.

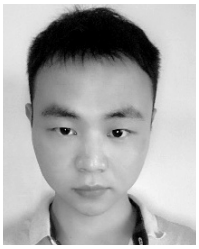

BIN ZHOU was born in Xinyang, Henan, China, in 1991. He received the B.S. and M.S. degrees in aeronautical engineering from Air Force Engineering University, Xi'an, Shaanxi, China, in 2015, where he is currently pursuing the Ph.D. degree in aerospace engineering with the Aeronautics and Astronautics Engineering Institute.

His main research interests include aero-engine control systems, networked control systems, sliding mode control, and robust control.

SHOUSHENG XIE was born in Yunan, Guangdong, China, in 1959. He received the B.S. and M.S. degrees from Air Force Engineering University, Xi'an, Shaanxi, China, in 1985, and the Ph.D. degree from Northwestern Polytechnical University, Xi'an, in 1998, all in aerospace engineering.

He is currently a Professor with the Department of Aeronautical Engineering, Air Force Engineering University. He is the author of seven books, more than 100 articles, and holds 14 patents. His research interests include the aircraft propulsion system integrated control, networked control systems, distributed control, and fault diagnosis.

JUNHUA HUI was born in Xi'an, Shaanxi, China, in 1990. She received the B.S. and M.S. degrees in aeronautical engineering from Air Force Engineering University, Xi'an, in 2013.

She is currently a Lecturer with the Department of College of Information and Communication, National University of Defense Technology. She is the author of the book *Knowledge Representation and Processing* and more than ten articles. Her research interests include artificial intelligence, networked control systems, and information service.